Molecular Therapy
Nucleic Acids
Original Article

Downregulation of Hypoxia-Inducible Factor-1α by RNA Interference Alleviates the Development of Collagen-Induced Arthritis in Rats

Yiping Hu,[1,2] Tiantian Zhang,[3] Jingqin Chen,[1,4] WenXiang Cheng,[1,4] Jianhai Chen,[1,4] Zhengtan Zheng,[1] Jietao Lin,[1,4] Guoyuan Zhu,[6] Yong Zhang,[7] Xueling Bai,[1] Yan Wang,[1] Bing Song,[9] Qingwen Wang,[2] Ling Qin,[8] and Peng Zhang[1,4,5]

[1]Center for Translational Medicine Research and Development, Shen Zhen Institutes of Advanced Technology, Chinese Academy of Science, Shenzhen, Guangdong 518055, China; [2]Department of Rheumatism and Immunology, Peking University Shenzhen Hospital, Shenzhen, Guangdong 518036, China; [3]Department of Rheumatology, People's Hospital of Bao'an District, Shenzhen, Guangdong 518128, China; [4]University of Chinese Academy of Sciences, Beijing 10049, China; [5]University of Chinese Academy of Sciences, Shenzhen Hospital, Shenzhen 518000, China; [6]State Key Laboratory of Quality Research in Chinese Medicine, Macau Institute for Applied Research in Medicine and Health, Macau University of Science and Technology, Macau, China; [7]Shenzhen Pingle Orthopaedic Hospital, Guangdong 518000, China; [8]Musculoskeletal Research Laboratory of Department of Orthopaedics & Traumatology, The Chinese University of Hong Kong, Hong Kong SAR, China; [9]School of Dentistry, Cardiff University, Cardiff, Heath Park, CF23 6AL Wales, UK

Rheumatoid arthritis (RA) is the most common type of autoimmune arthritis. Hypoxia-inducible factor-1α (HIF-1α) as a transcription factor in response to hypoxia suggests that it could be a potential therapeutic target for the treatment of RA. In this study, we assessed whether the HIF pathway blockade attenuates the manifestations of RA in the collagen-induced arthritis (CIA) rat model. We constructed a short hairpin RNA (shRNA) lentiviral expression vector targeting HIF-1α (pLVX-shRNA-HIF-1α) and to achieve HIF-1α RNA interference. Quantitative RT-PCR, immunofluorescence staining, and western blot were used to detect the expressions of HIF-1α, vascular endothelial growth factor (VEGF), phsopho (p)-p65, and p-IKBα mRNA and protein, respectively. Micro-computed tomography was used to investigate joint morphology at different time points after CIA induction. Moreover, enzyme-linked immunosorbent assay (ELISA) was used to monitor the expression of inflammatory cytokines. *In vitro* analyses revealed that pLVX-shRNA-HIF-1α effectively inhibited the expression of HIF-1α and VEGF and led to the activation of p-65 and p-IKBα, as well as decreased proinflammatory cytokine expression in cell culture. Inhibition of HIF-1α in rats decreased signs of a systemic inflammatory condition, together with decreased pathological changes of RA. Moreover, downregulation of HIF-1α expression markedly reduced the synovitis and angiogenesis. In conclusion, we have shown that pharmacological inhibition of HIF-1 may improve the clinical manifestations of RA.

INTRODUCTION

Rheumatoid arthritis (RA) is a chronic, progressive disorder that is characterized by synovial tissue proliferation and joint inflammation, ultimately causing the destruction of articular cartilage and subchondral bone.[1–3] The current view is that inflammatory cytokines play an essential role in the RA process, and the nuclear factor kappa-B (NF-κB) signaling pathway is one of the most important pathways included.[4–6] Both tumor necrosis factor α (TNF-α) and interleukin (IL)-1 are critical mediators of the inflammatory response in RA. Clinical trials of anti-TNF-α/IL-1 reagents have demonstrated the therapeutic efficacy in cases of RA.[2,7,8] There is growing evidence supporting the notion that hypoxia is the critical effector for both inflammatory and destructive responses in RA. It has been reported that hypoxia is crucial for the development and persistence of RA in both animals and humans.[9,10]

More recent research indicated that hypoxia, due to elevated oxygen consumption by infiltrated myeloid cells, is the main feature of inflamed tissue.[11,12] The typical pathological symptoms of early-stage RA are changed vascular density and increased neovascularization and followed by chronic inflammation and bone destruction. In this process, hypoxia acts as a major regulator of inflammatory mediators.[13] Hypoxia-inducible factor-1 (HIF-1) is a major mediator that adapts to hypoxia. The HIF-1 heterodimer is composed of two helix-loop-helix proteins, namely, HIF-1α and HIF-1β.[14,15] HIF-1α is the key transcriptional factor in a hypoxic response. Previous studies have demonstrated that the synovium of patients with RA demonstrates a hypoxic nature and presents HIF-1α upregulation.[16,17]

Received 23 October 2019; accepted 10 January 2020;
https://doi.org/10.1016/j.omtn.2020.01.014.

Correspondence: Peng Zhang, Center for Translational Medicine Research and Development, Shen Zhen Institutes of Advanced Technology, Chinese Academy of Science, Shenzhen, Guangdong 518055, China.
E-mail: peng.zhang@siat.ac.cn
Correspondence: Ling Qin, Musculoskeletal Research Laboratory of Department of Orthopaedics & Traumatology, The Chinese University of Hong Kong, Hong Kong SAR, China.
E-mail: qin@ort.cuhk.edu.hk
Correspondence: Qingwen Wang, Department of Rheumatism and Immunology, Peking University Shenzhen Hospital, Shenzhen, Guangdong 518036, China.
E-mail: wqw_sw@163.com

Under hypoxic conditions, HIF-1α is activated and stably expressed, accumulates in the nucleus and then binds with other hypoxic response elements to form a conformer.[18] HIF-1α and the constitutively expressed aryl hydrocarbon receptor nuclear translocator activate and migrate to the nucleus, where it binds to HIF-1β to form the complex; the complex binds to hypoxia-responsive elements and active hypoxia response genes that mainly mediate cell proliferation, angiogenesis, and migration.[13,19]

In addition, HIF-1α activation is upregulated by a variety of inflammatory factors, such as, TNF-α, IL-1β, and IL-33, which are overexpressed in RA synovial fibroblasts, but the underlying molecular mechanism of action remains unclear.[20,21] HIF-1α is activated, and mass production-enhanced RA synovial fibroblasts mediate the expansion of inflammatory T cells, causing the further overexpression of proinflammatory cytokines, such as interferon-γ (IFN-γ) and IL-17.[16,22] The above pathogenic mechanisms indicate a vicious cycle that ultimately leads to severe RA development.

Lee et al.[23] have silenced HIF-1α by short interfering RNA (siRNA) in rheumatoid synovial fibroblasts and found hypoxia in arthritic joints may induce the differential expression of matrix metalloproteinase-1 (MMP-1) and MMP-13 in a HIF-1α-dependent manner in rheumatoid synovial fibroblasts during joint inflammation. This indicates that HIF-1α controls the genes in bone destruction in RA, which can be used as an effective therapeutic target. siRNA interference therapy is one of the more widely used gene therapy methods. In this study, the exogenous short hairpin structure of the interfering RNA (short hairpin RNA [shRNA]) fragment of HIF-1α was constructed on a lentiviral vector. Gene recombinant technology was used to obtain lentivirus particles stably expressing HIF-lα-shRNA (pLVX-HIF-lα-shRNA). The effect of lentivirus-mediated shRNA on the target gene HIF-1α and its related genes was determined in cell-based experiments. Animal experiments were also conducted to evaluate the therapeutic efficacy of our novel pLVX-HIF-lα-shRNA for RA.

RESULTS

HIF-1α and VEGF Expression Analysis *In Vitro*

The expression of HIF-1α and vascular endothelial growth factor (VEGF) mRNA in the pLVX-shRNA-HIF-1α group was significantly (4.7- and 2.8-fold) lower than that in the collagen-induced arthritis (CIA) synovial cells without transfection group (CSC) and pLVX-shRNA-conHIF-1α groups ($p < 0.01$) (Figures 1A and 1B). No statistical difference was found between the CSC and pLVX-shRNA-conHIF-1α groups (Figures 1A and 1B). Western blot results showed that the protein expression bands of HIF-1α and VEGF were significantly lower in the synovial cells of the pLVX-shRNA-HIF-1α group than in those of the CSC and pLVX-shRNA-conHIF-1α groups (Figure 1C). This indicates that pLVX-shRNA-HIF-1α can significantly silence target gene expression at the protein level. Further study demonstrated that decreased inflammation in the pLVX-shRNA-HIF-1α group was used as a marked activation of NF-κB signaling, as detected by a remarkable reduction in phospho (p)-IKBα and p-NF-κB/p65 in the synovial cell (Figure 1D), indicating that the loss of HIF-1α may inhibit joint inflammation and NF-κB activation.

The results of immunofluorescence showed that the fluorescence intensity of HIF-1α and VEGF proteins was significantly lower in the pLVX-shRNA-recombinant (r)HIF-1α group than in the CSC and the pLVX-shRNA-conHIF-1α groups (Figures 1E and 1F).

Cytokine Concentration in Cell Culture Supernatant and Peripheral Blood Serum

Enzyme-linked immunosorbent assay (ELISA) detected related inflammatory factors in cell culture supernatant and serum: TNF-α, IL-1β, and IL-6. The concentrations of TNF-α in the cell culture supernatant after virus infection were 2.6-fold in the CSC and 1.9-fold in the pLVX-shRNA-HIF-1α groups lower than in the pLVX-shRNA-conHIF-1α group ($p < 0.01$) (Figure 1G). The concentrations of IL-1β in the cell culture supernatant after virus infection were 1.9-fold in the CSC and 1.8-fold in the pLVX-shRNA-HIF-1α groups lower than in the pLVX-shRNA-conHIF-1α group ($p < 0.01$) (Figure 1H). The concentrations of IL-6 in the cell culture supernatant after virus infection were 1.61-fold in the CSC and 1.3-fold in the pLVX-shRNA-HIF-1α groups lower than in the pLVX-shRNA-conHIF-1α group ($p < 0.01$ and $p < 0.05$) (Figure 1I). In the inflammatory factors in serum, at 7 and 14 days after treatment, results showed that the expression of inflammatory factors TNF-α in the pLVX-shRNA-HIF-1α group was 1.76-fold and 1.82-fold, reduced 7 days after administration compared with the pLVX-shRNA-conHIF-1α and phosphate-buffered saline (PBS) groups ($p < 0.01$) (Figure 1J). The expression of inflammatory factors IL-1β in the pLVX-shRNA-HIF-1α group was 2.10-fold and 2.13-fold reduced, 7 days after administration, compared with the pLVX-shRNA-conHIF-1α and PBS groups ($p < 0.01$) (Figure 1K). The expression of inflammatory factors IL-6 in the pLVX-shRNA-HIF-1α group was 1.3-fold and 1.28-fold, reduced 7 days after administration, compared with the pLVX-shRNA-conHIF-1α and PBS groups ($p < 0.05$) (Figure 1L). The expression levels of TNF-α 1.83-fold and 1.84-fold decreased in the pLVX-shRNA-HIF-1α group compared with the pLVX-shRNA-conHIF-1α and the PBS groups at 14 days after administration ($p < 0.01$) (Figure 1J). The expression levels of IL-1β 1.76 -fold and 1.79-fold decreased in the pLVX-shRNA-HIF-1α group compared with the pLVX-shRNA-conHIF-1α and the PBS groups at 14 days after administration ($p < 0.01$) (Figure 1K). The expression of IL-6 in the pLVX-shRNA-HIF-1α group decreased after 14 days of administration, but no statistical difference was found compared with the pLVX-shRNA-conHIF-1α and the PBS groups (Figure 1L).

X-Ray and Micro-CT Measurement

Results showed that the entire joints of the pLVX-shRNA-conHIF-1α and the PBS groups were severely damaged. The complete joint structure was difficult to observe, and the joint adhesion had no obvious joint space. Joint destruction in the pLVX-shRNA-HIF-1α group was suppressed, and joint structure and joint space were clearly observed (Figure 2A). The X-ray scores of the pLVX-shRNA-HIF-1α group were 2.27-fold and 2.33-fold lower than those

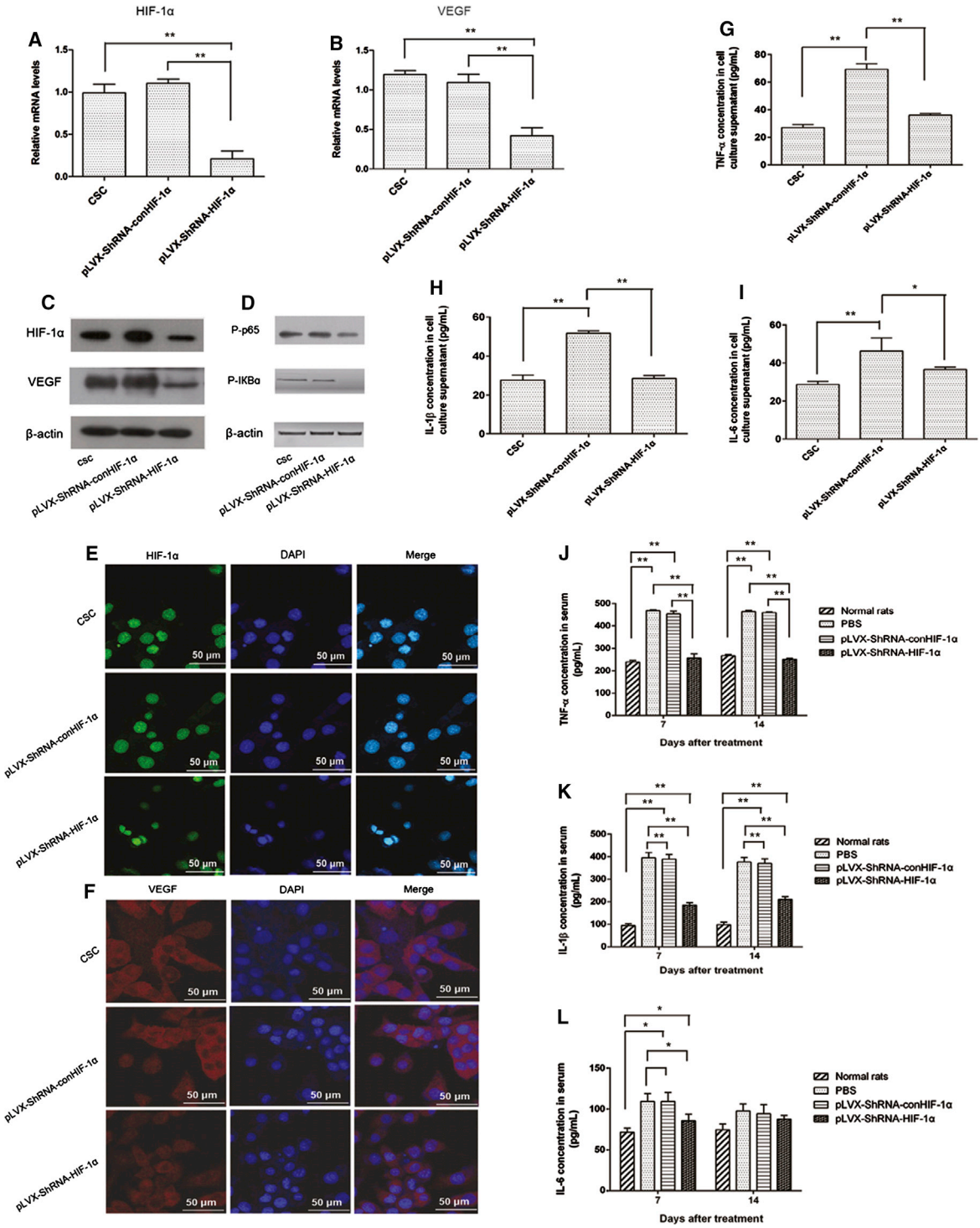

Figure 1. Detection of Silencing Effect of pLVX-shRNA-Puro-HIF-1α on HIF-1α and VEGF Expression in a Synovial Cell

(A) HIF-1α mRNA expression. (B) VEGF mRNA expression. (C) Western blot detection of HIF-1α and VEGF protein expression. (D) Western blot detection of p-p65 and p-IKBα protein expression. Immunofluorescence detection of HIF-1α and VEGF expression in synoviocytes. (E) HIF-1α fluorescence expression. (F) VEGF fluorescence expression. ELISA detects the concentration of related inflammatory factors. (G) The concentration of TNF-α in CIA synovial cell culture supernatant. (H) The concentration of IL-1β in CIA synovial cell culture supernatant. (I) The concentration of IL-6 in CIA synovial cell culture supernatant. (J) The concentration of TNF-α in serum at 7 and 14 days after treatment. (K) The concentration of IL-1β in serum at 7 and 14 days after treatment. (L) The concentration of IL-6 in serum at 7 and 14 days after treatment (*$p < 0.05$, **$p < 0.01$).

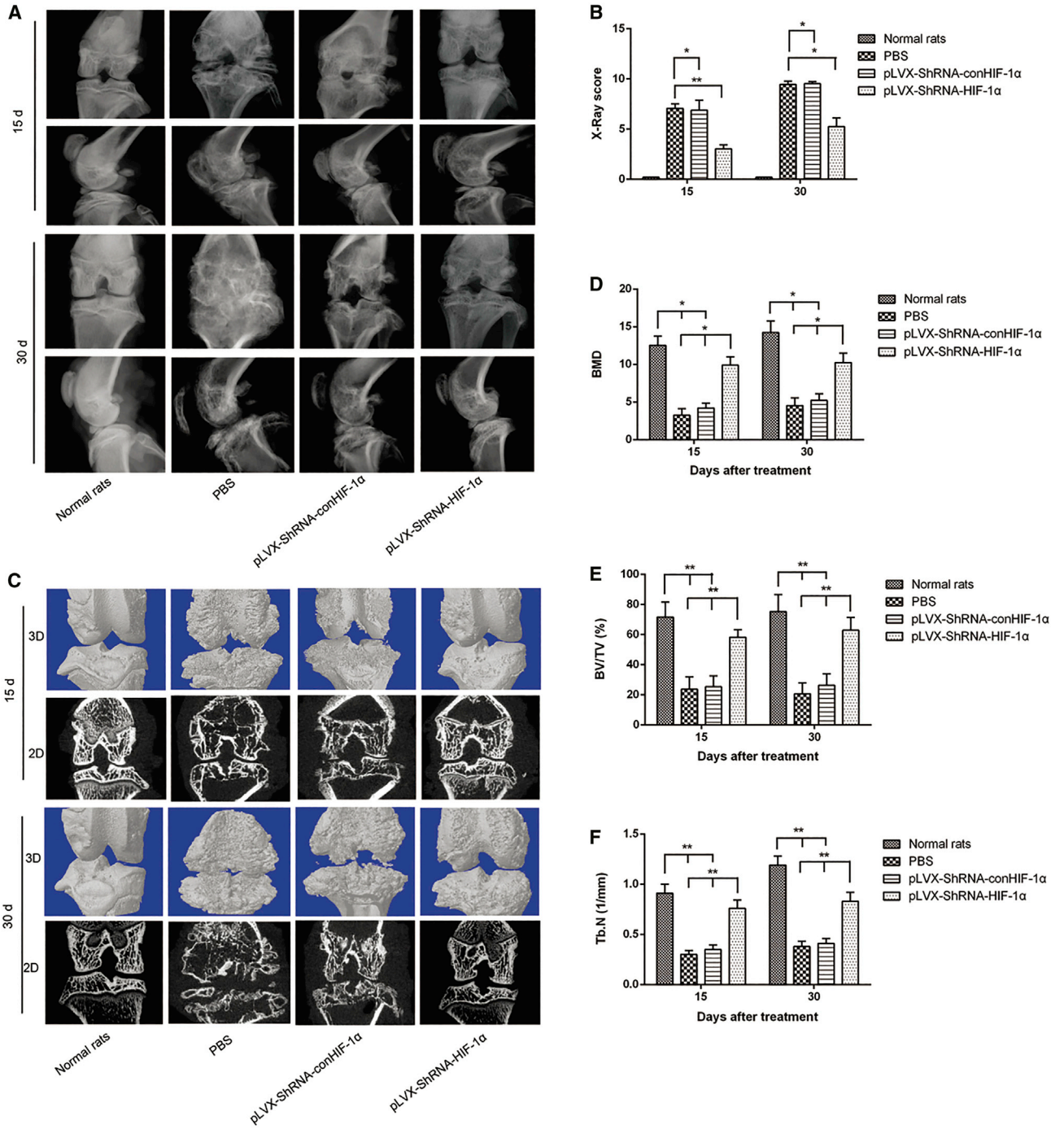

Figure 2. X-Ray Analyses after 15 and 30 Days of Drug Administration to Assess Joint Destruction and Semiquantitative Integration Statistics

(A) Results of X-ray analyses. (B) X-ray semiquantitative analysis results. Micro-CT analysis joint structure scan and quantitative statistics. (C) 2D and 3D joint structure images. (D) Bone mineral density (BMD). (E) The ratio of bone volume to tissue volume (BV/TV). (F) Trabecular number (Tb. N) (*$p < 0.05$, **$p < 0.01$, $n = 5$).

of the pLVX-shRNA-conHIF-1α and PBS groups 15 days after treatment and 1.81-fold and 1.80-fold lower than those of the pLVX-shRNA-conHIF-1α and PBS groups 30 days after treatment (Figure 2B).

Bone quality and quantitative analysis were performed by micro-computed tomography (micro-CT) analysis, 15 and 30 days after treatment. CT scans were performed with 2D and 3D image reconstructions using SkyScan analysis software. Joint destruction was clearly visible in

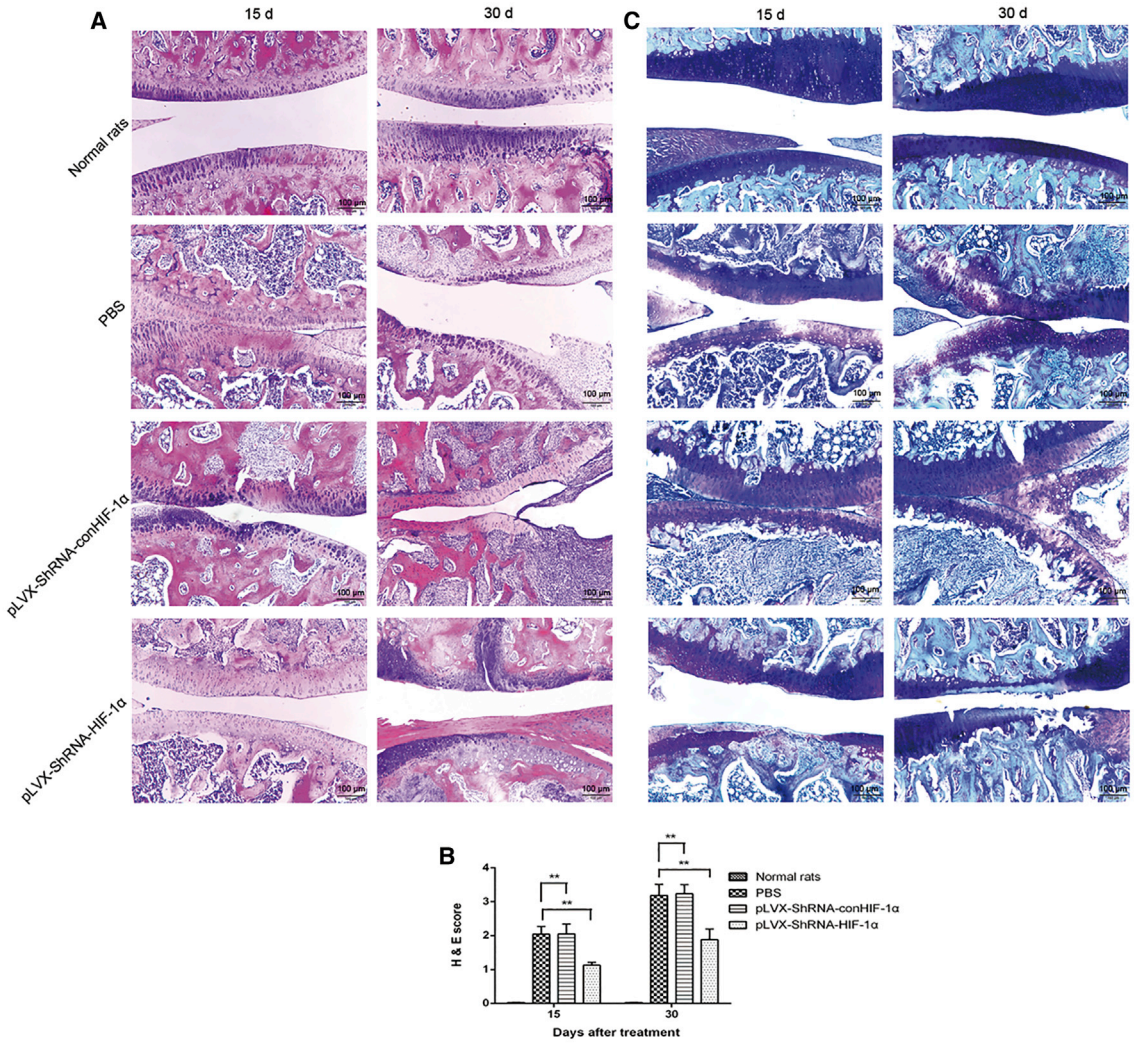

Figure 3. Synovial Tissue Inflammation and Bone Destruction Observed by H&E Staining and Semiquantitative Analysis

(A) H&E staining. (B) H&E semiquantitative integral. (C) Articular cartilage toluidine blue staining detection (**$p < 0.01$, $n = 5$).

the pLVX-shRNA-conHIF-1α and the PBS groups (Figure 2C). Quantitative analysis showed that bone mineral density (BMD) was 2.33-fold and 3.03-fold reduced in the pLVX-shRNA-conHIF-1α and the PBS groups compared with the pLVX-shRNA-HIF-1α group 15 days after treatment and 1.95-fold and 2.25-fold reduced in the pLVX-shRNA-conHIF-1α and the PBS groups compared with the pLVX-shRNA-HIF-1α group 30 days after treatment ($p < 0.05$) (Figure 2D). Quantitative analysis showed that bone volume to tissue volume (BV/TV) was 2.31-fold and 2.47-fold higher in the pLVX-shRNA-HIF-1α group than in the pLVX-shRNA-conHIF-1α and the PBS groups 15 days after treatment and 2.39-fold and 3.06-fold higher in the pLVX-shRNA-HIF-1α group than in the pLVX-shRNA-conHIF-1α and the PBS groups 30 days after treatment ($p < 0.01$) (Figure 2E). Quantitative analysis showed that trabecular number (Tb. N) was 2.17-fold and 2.53-fold higher in the pLVX-shRNA-HIF-1α group than in the pLVX-shRNA-conHIF-1α and the PBS groups 15 days after treatment and 2.02-fold and 2.18-fold higher in the pLVX-shRNA-HIF-1α group than in the pLVX-shRNA-conHIF-1α and the PBS groups 30 days after treatment ($p < 0.01$) (Figure 2F).

Histological Analyses

The inflammatory cell infiltration in the articular cartilage surface as well as the cartilage and subchondral bone destruction were severe in the pLVX-ShRNA-conHIF-1α and PBS groups. However, the destruction of articular cartilage and subchondral bone in the pLVX-ShRNA-HIF-1α group was significantly improved (Figure 3A). Statistical integration showed that the hematoxylin and eosin (H&E) score of the pLVX-shRNA-HIF-1α group was 1.82-fold and 1.80-fold lower than that of the pLVX-shRNA-conHIF-1α and PBS groups 15 days after treatment and 1.72-fold and 1.69-fold lower than that of the pLVX-shRNA-conHIF-1α and PBS groups 30 days after treatment ($p < 0.01$) (Figure 3B).

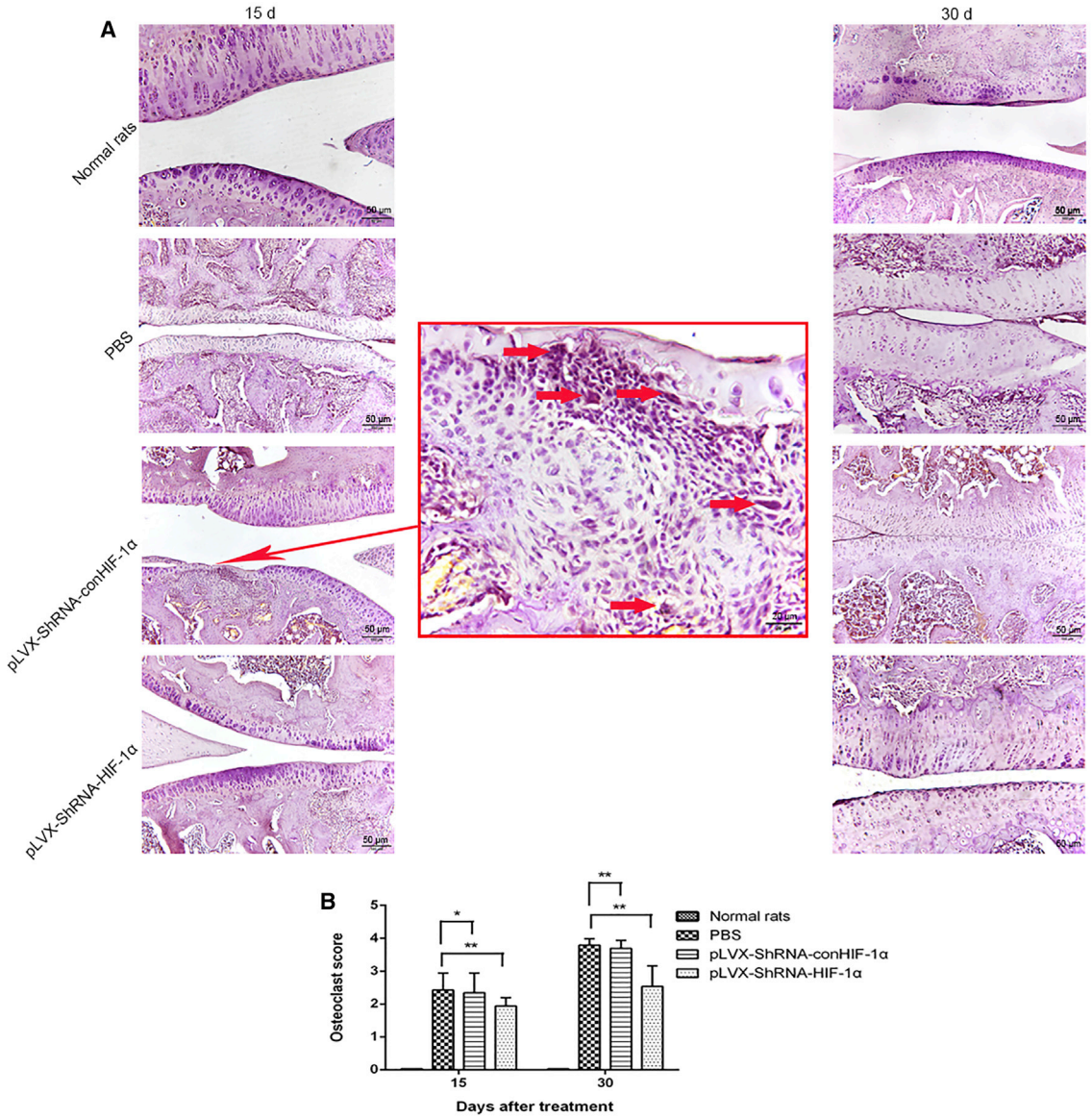

Figure 4. Analysis of Osteoclasts and Pannus Staining and Quantitative Analysis in Joints

The red box is the enlarged region, and the red arrows are osteoclasts. (A) Tissue sections were stained with TRAP to examine osteoclast at different time points. (B) Statistical data of osteoclast score in the fracture area of different groups (*$p < 0.05$, **$p < 0.01$, $n = 5$).

The articular cartilage surface and the subchondral bone surface of the pLVX-shRNA-conHIF-1α and PBS groups were severely damaged. The articular chondrocytes were hypertrophied, and the pathological fusion between the joints was severe. Pathological damage of cartilage in the pLVX-shRNA-HIF-1α group was significantly improved (Figure 3C).

A large number of osteoclasts were present in the pLVX-shRNA-conHIF-1α and PBS groups, accompanied by a large number of pannus formation. By contrast, the number of osteoclasts and the area of pannus in the pLVX-shRNA-HIF-1α group significantly improved (Figure 4A). Statistical integration showed that the osteoclast scores in the pLVX-shRNA-HIF-1α group were 1.21-fold and 1.25-fold lower than those in the pLVX-shRNA-conHIF-1α and PBS groups at 15 days after treatment and 1.46-fold and 1.49-fold lower than those in the pLVX-shRNA-conHIF-1α and PBS groups at 30 days after treatment (Figure 4B).

Immunohistochemical Analysis of HIF-1α and VEGF Protein Expression *In Vivo*

VEGF and HIF-1α were significantly expressed in the synovial membrane and bone-destruction sites of the pLVX-shRNA-conHIF-1α and PBS groups compared with the pLVX-shRNA-HIF-1α group

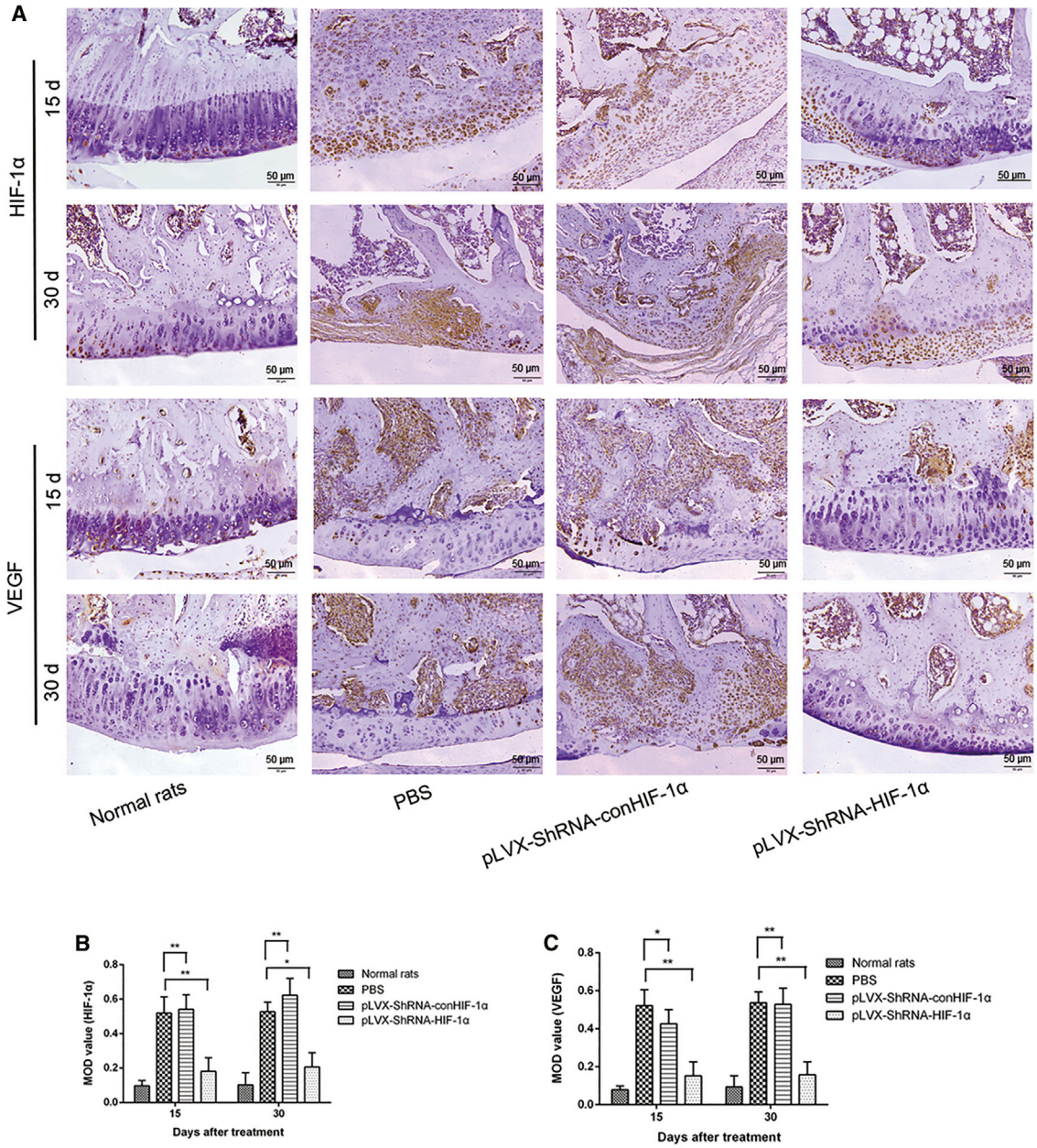

Figure 5. Expression and Quantitative Analysis of HIF-1α and VEGF by Immunohistochemical Staining

(A) Immunohistochemical staining results of HIF-1α and VEGF. (B) HIF-1α immunohistochemical mean optical density (MOD) integration results. (C) VEGF immunohistochemical MOD integration results (*$p < 0.05$, **$p < 0.01$, $n = 5$).

(Figure 5A). The positive mean optical density (MOD) values of the positive cells showed that the expression levels of HIF-1α were 2.97-fold and 2.85-fold lower in the pLVX-shRNA-HIF-1α group than in the pLVX-shRNA-conHIF-1α and PBS groups 15 days after treatment and 3.01-fold and 2.54-fold lower in the pLVX-shRNA-HIF-1α group than in the pLVX-shRNA-conHIF-1α and PBS groups 30 days after treatment ($p < 0.01$ and $p < 0.05$) (Figure 5B). The positive MOD values of the positive cells showed that the expression levels of VEGF were 2.80-fold and 3.43-fold lower in the pLVX-shRNA-HIF-1α group than in the pLVX-shRNA-conHIF-1α and PBS groups 15 days after treatment and 3.36-fold and 3.41-fold lower in the pLVX-shRNA-HIF-1α group than in the pLVX-shRNA-conHIF-1α and PBS groups 30 days after treatment ($p < 0.01$ and $p < 0.05$) (Figure 5C). In the expression levels of HIF-1α and VEGF, no significant differences were found between the pLVX-shRNA-HIF-1α and normal animal groups (Figures 5B and 5C).

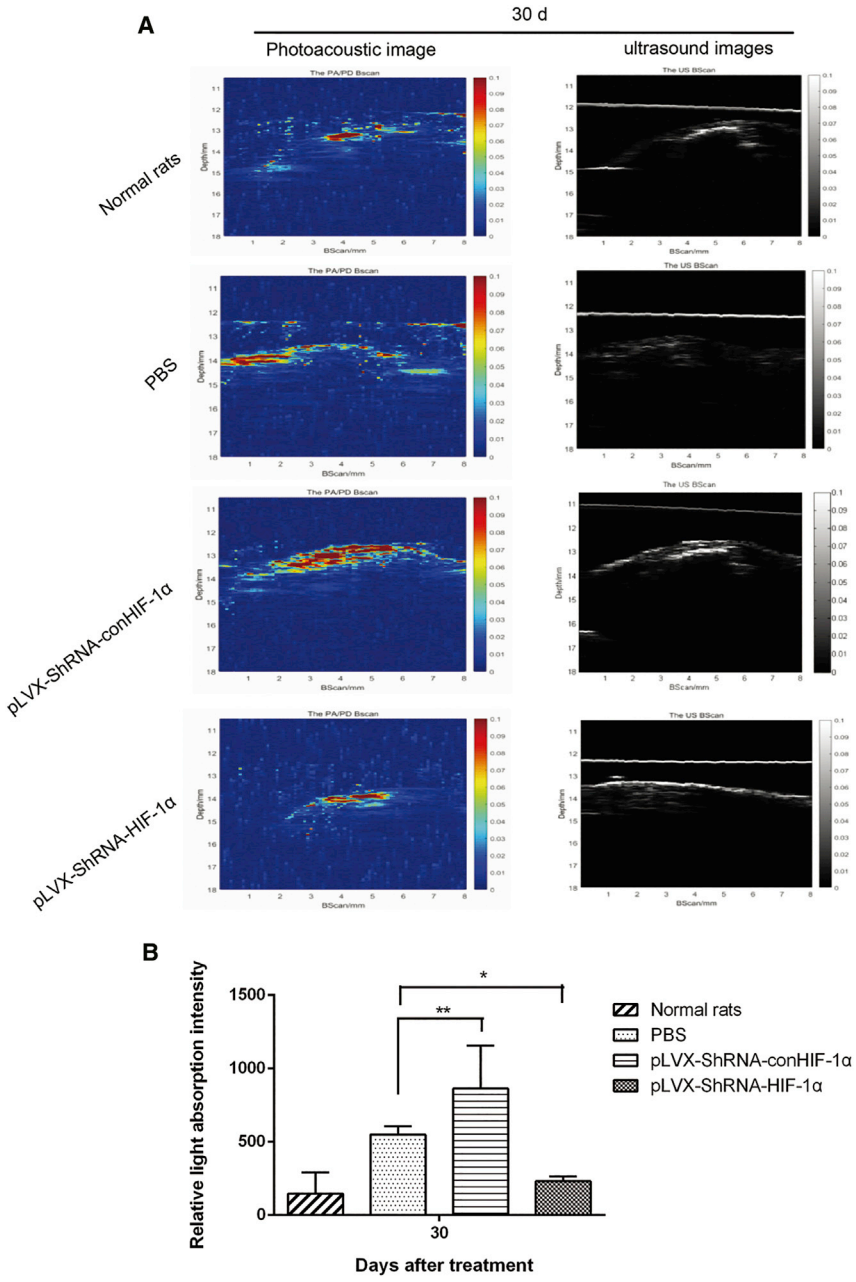

Figure 6. Multiscale Photoacoustic Imaging for Neovascularization

(A) CIA rat model ankle-joint photoacoustic imaging. (B) Semiquantitative analysis of relative light absorption intensity (*$p < 0.05$, **$p < 0.01$, $n = 5$).

DISCUSSION

The highly dysregulated architecture of the microvasculature creates a hypoxia supply to the synovium; activation of immune inflammatory cells has been mediated by the proinflammatory signal HIF-1α,[24] so we hypothesized that silencing HIF-1α plays a key role in the development of RA. HIF-1α is regulated by multiple factors at the transcriptional and post-transcriptional levels and is a complex process. RNA interference has been a mature technology after years of development; it can be used to silence the expression of any disease-related transcribed genomic sequence in a selective and sequence-dependent manner.[25,26] There is growing evidence supporting the notion that synovial cells play important roles in both inflammatory and destructive responses in RA.

As synovial cells have been demonstrated to participate in almost all of the pathological events and play an important role in RA pathogenesis, we isolated the synovial cells of CIA for *in vitro*-related studies. RA synovial tissue natural hypoxia was first measured in the synovial fluid sample of RA patients by the Clark electrode in 1970.[27] For a further step, HIF-1α was found to play an important role in the pathology of RA by regulating the angiogenesis and expression of inflammatory factors.[23,28,29] Moreover, Hollander et al.[30] have demonstrated HIF-1α stabilization in the RA joint synovial tissue but not in nonarthritic synovia or in most osteoarthritis (OA) synovia. Therefore, HIF-1α plays a role of a potential therapeutic target for the treatment of RA by using RNA interference.

In the pathogenesis of RA, changes in articular cartilage are important characteristics. The normal articular cartilage tissue is transparent with a smooth surface and is mainly composed of chondrocytes and cartilage matrix without blood vessel and nerve structure inside.[31,32] In addition, the gap narrow is not obvious, and the amount of proliferation of the articular surface is small.[32] Long-term inflammation erodes articular cartilage and subchondral bone, causing articular cartilage to become thin, sticky, and disrupted, whereas subchondral bone is fibrotic and causes osteoporosis. Multiple joints and tissues are involved until the joint function is lost.[33,34] In our research, micro-CT and X-ray results showed that the joint destruction of

Multiscale Photoacoustic Imaging Angiogenesis Analysis

Multiscale photoacoustic (PA) imaging scans of the ankle joint were evaluated 30 days after treatment. The angiogenic signal (red and yellow display in the Figure 6A) of the pLVX-shRNA-HIF-1α group was lower than that of the pLVX-shRNA-conHIF-1α and PBS groups (Figure 6A). Statistical semiquantitative analysis showed that the relative absorbance intensity of PA was 3.76-fold and 2.39-fold lower in the pLVX-shRNA-HIF-1α group than in the pLVX-shRNA-conHIF-1α and PBS groups 30 days after treatment ($p < 0.01$ and $p < 0.05$; Figure 6B).

the group with effective silencing of the target gene HIF-1α significantly improved, and the narrowing of the joint space was controlled. The results of histological staining also showed that the articular cartilage was severely damaged in the negative-treatment group and control group, with a large number of pannus and osteoclasts appearing in the subchondral bone. This condition greatly improved after RNA interference treatment.

As we mentioned above, inflammation initially erodes the synovial membrane around the joint and gradually leads to the destruction of both cartilage and subchondral bone.[35–37] At present, nonsteroidal anti-inflammatory drugs (NSAIDs) and disease-modifying anti-rheumatic drugs (DMARDs) are the first choice for the therapy of RA because they play a vital role in inhibiting inflammation and controlling pathological progress.[38,39] However, new therapeutic methods for the treatment of RA should be developed to avoid the side effects of NSAIDs and DMARDs. With the development of biotechnology and drug technology, increasing attention has been paid to biotherapy agents that target genes, potentially triggering human diseases. In the present study, we focused on whether HIF-1α mediates inflammatory cell production and activation of inflammatory signals. We found that serum inflammatory factor concentration, western blot detection of p-p65 and p-IKBα protein expression, tartrate-resistant acid phosphate (TRAP) staining, and H&E staining showed that the group with effective silencing of the target gene HIF-1α demonstrated significantly reduced concentration of inflammatory factors and number of osteoclasts, effectively inhibiting pathological development of the CIA model.

Vascular growth is a typical feature in the inflammatory synovial tissue of early and confirmed RA.[1,40,41] Angiogenesis is a complex process that is affected by many factors, and VEGF is a key regulator of angiogenesis during inflammation.[42,43] VEGF is also a product of the synovial membrane response to hypoxia and proinflammatory factors invading the pathological environment.[42,44,45] In our research, VEGF immunohistochemical staining and multiscale PA vascular analysis results showed that the group with effective silencing of the target gene HIF-1α demonstrated significantly reduced VEGF expression and angiogenesis signals, which indicate the therapeutic effect of RNA interference in another side as well.

In summary, pLVX-ShRNA-HIF-1α screened by *in vitro* cells can effectively silence the target gene HIF-1α. The pharmacological effects of pLVX-ShRNA-HIF-1α on the rat CIA model were determined. Results indicated that pLVX-ShRNA-HIF-1α can effectively inhibit inflammation protein expression and vascular proliferation and significantly improve the destruction of articular cartilage and subchondral bone in CIA rats. These results indicate that HIF-1α can be used as a target for the regulation of angiogenesis and the potential treatment of RA. The potential clinical translation of this method still needs a long time to process. Also, to determine whether it is effective in the clinic, a nonhuman primate animal model is needed.

MATERIALS AND METHODS

Animals

Fifty female Wistar rats, 10 weeks of age, were purchased from Beijing Vital River Laboratory Animal Technology (Beijing, China). The animals were fed in a specific pathogen-free facility at the Shenzhen Institute of Advanced Technology, Chinese Academy of Science. The experimental protocol was approved by the Laboratory Animal Ethical and Welfare Committee of the Shenzhen Institute of Advanced Technology, Chinese Academy of Science (no: SIAT-IRB-170302-YGS-A0285).

Construction of si-HIF-1α Plasmid

Rat HIF-1α mRNA (GenBank: NM_024359) was employed as the template strand, and an online shRNA design tool was used to obtain the target gene interference sequence (http://rnaidesigner.thermofisher.com/rnaiexpress/sort.do). In this study, we designed three HIF-1α target sequences to construct the lentiviral shRNAs and negative sequence selected as a control (Supplemental Methods). shRNA fragments were synthesized by Invitrogen (Shanghai, China), and an Xhol cleavage site was inserted at the 3′ end of shRNA. The targeting sequence synthesizes two complementary nucleic acid strands and was cloned into the target vector pLVX/U6/Green fluorescent protein (GFP). Then, they were confirmed by specific enzyme digestion and agarose gel electrophoresis by sequencing nucleic acids (Figures S1 and S2). The correct vector plasmid packaging virus was identified. The lentiviral shRNA-expressing plasmids pLVX-shRNA2-puro, Amp^+ (Biowit Technology, Shenzhen, China) were transfected with the packaging plasmids into 293T cells for lentivirus generation (Figure S3). The viral supernatants were harvested, and 293T cells were used to determine the titer of viral biological activity. The titers of the lentiviruses were generally up to 10^8 transduction units (TU)/mL (Figure S4).

Induction of Collagen-Induced Arthritis (CIA) in Wistar Rats and shRNA Treatment Regiment

Forty rats were immunized to induce arthritis with collagen type II (20022; Chondrex; dissolved in 0.05 M acetic acid) and incomplete Freund's adjuvant (IFA; 7002; Chondrex). The method was followed as per the Brand et al.[46] publication. Rats were observed three times a week by the same experimenter to determine the presence of arthritis and were identified as CIA when erythema and swelling were obviously observed, at least on the digits and/or paws.

Fifty rats were used in this study. Arthritis was present in 34 of 40 immunized rats 14 days after secondary immunization. After the onset of arthritis, the rats were divided into four groups (n = 10) as follows: an shRNA interference plasmid group (pLVX-shRNA-HIF-1α), a negative control shRNA plasmid group (pLVX-shRNA-con-HIF-1α), a PBS group, and normal rats as the control group. *In vitro* experiments were screened for effective lentiviral vector mediated with shRNA virus (concentration of 1 × 108 TU/mL) and injected into the knee-joint and ankle-joint cavity of the CIA model animal. Two injections each with a dose of 0.1 mL were

administered per week for 2 weeks. The same method of operation was performed in the other control group. After the administration was finished, five rats in each group were selected for each efficacy index test at 15 and 30 days.

Cell Culture and shRNA Infection

The synovial cells were isolated according to the previous studies. Briefly, immediately after euthanasia, the synovial tissue was extracted from the knee of the CIA model and placed in sterile phosphate buffered saline (PBS). Synovial tissues were cut into 1- to 2-mm^3 pieces (specimens were soaked in PBS throughout the procedure). The shredded tissue pieces were transferred to a 35-mm-diameter Petri dish. A 4-mL volume of 0.4% type I collagenase (Sigma) was added to the Petri dish and was digested in a 5% CO_2 clean incubator at 37°C for 4 h. Then, the tissue was filtered and centrifuged to obtain synovial cells. The cells were continuously cultured in the incubator for 24 h, the adherent cells were primary synovial cells, and the unattached cells were discarded. The cells were placed in DMEM containing 10% fetal bovine serum and then incubated.

CIA synovial cells were maintained in DMEM and plated into six-well plates at 1×10^6 cells/well. Cells were assigned into the following groups: CSC, transfected with shRNA interference plasmid group (pLVX-shRNA-HIF-1α), and transfected negative control shRNA plasmid group (pLVX-shRNA-conHIF-1α). After 24 h, the cells were infected with viral supernatant (50 μL, 10^8 TU/mL) in the presence of polybrene (8 μg/mL final concentrations) for 24 h at a multiplicity of infection (MOI) of 20 and then added to a fresh DMEM medium. After 48 h, the cells were collected and stored under suitable conditions for later experiments.

For ELISA detection of the inflammatory cytokines in the cell culture supernatant, CIA synovial cells were maintained in DMEM and were plated into 6-well plates at 1×10^6 cells/well. 24 h later, 10 ng/mL TNF-α was added and incubated for another 4 h (the CSC group does not add TNF-α). After that, the medium was discarded and washed 2–3 times with PBS. Then, the cells were infected with supernatants, as described above. After 48 h, the cell supernatants were collected for ELISA (Neobioscience Technology, China).

Real-Time PCR Analysis

Total cell RNA was extracted using the Invitrogen RNA purification kit in accordance with the manufacturer's instructions. Real-time PCR reactions were performed in a LightCycler 96 system (Bio-Rad). Reaction cycle conditions were as follows: 50°C for 2 min and 95°C for 10 min of predenaturation conditions, 40 cycles at 95°C for 15 s and 60°C for 20 s and 72°C for 30 s. The primer sequences of the HIF-1α gene were as follows: forward primer, 5′-GTGGATATGTCTGGGTTGAG-3′; reverse primer, 5′-TTCTGTTTGTTGAAGGGAGA-3′; the product was 140 bp. The primer sequences of the VEGF were as follows: forward primer, 5′-TGTGAGCCTTGTTCAGAGCG-3′; reverse primer, 5′-GACGGTGACGATGGTGGTGT-3′; the product was 252 bp. The primer sequences of the *β-actin* standard control gene were as follows: forward primer, 5′-CGTTGACATCCGTAAAGACC TC-3′; reverse primer, 5′-TAGGAGCCAGGGCAGTAATCT-3′.

Western Blot Analysis

Radioimmunoprecipitation assay (RIPA) lysis and extraction buffer (Thermo Scientific; number 8900) were used to extract the total protein of CIA synovial cells. The same amount of protein was used to load and incubate the sample in a blocking solution for 1 h after electrophoresis to test HIF-1α, VEGF, phopsho-p65 (p-p65), phopsho-IKBα (p-IKBα), and β-actin protein. Protein samples were separated by 10% SDS-PAGE and transferred onto nitrocellulose membranes. The membranes were blocked with 5% nonfat milk overnight at 4°C, incubated with Tris-buffered saline/Tween 20 (TBST)-diluted primary antibodies (HIF-1α antibody: 1:800, ab1; VEGF antibody: 1:800, ab46154; p-p65 antibody: 1:600, ab97726; β-actin antibody: 1:2,000, ab20272 [Abcam, Cambridge, MA, USA]; p-IKBα antibody: 1:200, GTX32224 [Gene Tex]) at room temperature for 2 h, and then washed three times on the shaker for 10 min each time. The membranes were then incubated with secondary antibodies (1:2,500, ab6728; Abcam, Cambridge, MA, USA) at room temperature for 1 h and then washed three times with TBST on the shaker for 10 min each time. The test was purchased using a commercial enhanced chemiluminescence (ECL) luminescence kit (Nanjing Jiancheng Bioengineering Institute, China; w028-2).

Immunofluorescence Analysis

CIA synovial cells were cultured on glass coverslips, washed with PBS two times, and then fixed with 4% paraformaldehyde in PBS. The cells were then incubated with 3% bovine serum albumin blocking solution for 30 min at room temperature. The cells were stained with HIF-1α (1:1,000) and VEGF (1:500) antibodies overnight at 4°C and then incubated with fluorescein isothiocyanate (FITC)-conjugated secondary antibodies (1:1,000; Abcam, Cambridge, MA, USA; ab150117 and 150115) for 40 min at room temperature. After washing three times with PBS for 5 min each time, the nuclei were stained for 10 min with the fluorescent dye 4′,6-diamidino-2-phenylindole dihydrochloride (Sigma). The staining results were examined by confocal laser-scanning fluorescence microscopy (Leica, Germany; TCS SP5).

ELISA

Blood was collected at days 7 and 14 postinjection. Serum and cell culture supernatant collected in front of inflammatory factors, such as TNF-α, IL-1β, and IL-6, were detected using ELISA (Neobioscience Technology, China), in accordance with the manufacturer's instruction.

X-Ray Assessment

The radiological test (35 kV, 20 s; Faxitron, X-ray) was completed to evaluate the treatment effects of shRNA at days 15 and 30 postinjection. The semiquantitative integral analysis criteria are as follows:[47] 0 = normal joint structure and clearance; 1 = joint space is suspected to be narrowed, and the joint surface is slightly eroded; 2 = significantly

narrowed joint space and obvious articular surface erosion; 3 = blurred joint space, partial erosion of subchondral bone, and mild deformity of the articular surface; 4 = unrecognized joint space, most of the cartilage of the subchondral bone, and obvious structural abnormalities; and 5 = the entire joint contour is blurred, severely deformed, and accompanied by physical disability. All indicators of the scores were tested by two different experimenters, and the average of the two was the final result.

Micro-CT Analyses

At different time points (days 15 and 30) after treatment, micro-CT measurement was performed on the knee joint by using a model 1076 scanner (SkyScan, Bruker, Belgium). The detection parameter was 18 μm resolution, Al 1.0 mm filter, 60 kV voltages, and 400 μA current. The ratio of BV/TV, Tb. N, and BMD bone-related parameters were detected for all the samples.

Histological Staining Analyses

The rats were killed by overdosing with pentobarbital sodium. All samples were fixed in cold paraformaldehyde solution (4%) for 24 h and decalcified in 0.5 M EDTA neutral solution at room temperature for 45 days. Knee-joint paraffin sections (7 μm) were stained using an H&E staining kit (Nanjing Jancheng Technology). Toluidine blue (TB) staining was performed in accordance with to the manufacturer's instructions (Beijing Leagene Biotech). The criteria for semiquantitative evaluation of H&E are as follows:[48,49] 0 = normal joint synovial tissue and bone structure; 1 = synovial cell hypertrophy and inflammatory cell erosion of synovial tissue; 2 = cartilage destruction and pannus present; 3 = most articular cartilage and subchondral bone are destroyed; 4 = joint adhesions and stiffness and accompanying disability.

TRAP staining (Sigma) was performed to detect the expression of osteoclasts in accordance with the manufacturer's instructions. Semiquantitative analysis of TRAP staining was conducted in accordance with the following integral criteria:[48] 0 = no osteoclasts appeared; 1 = found a small amount of osteoclasts (lining fewer than 5% of most affected bone surfaces); 2 = a plurality of osteoclasts present in the field of view (lining 5%–25% of most affected bone surfaces); 3 = a large number of osteoclasts are present in the field of view (lining 30%–50% of most affected bone surfaces); and 4 = large-scale osteoclasts appear in the field of view (lining >50% of most affected bone surfaces). The scoring was completed by two experimenters, and the average was calculated. Above histologically stained sections were randomly selected for each rat, and six different views were observed for each section.

Immunohistochemical Analyses

Immunohistochemical staining for HIF-1α and VEGF proteins was completed. Samples were fixed in cold paraformaldehyde solution, decalcified, dehydrated, and then embedded in paraffin. The sections were subjected to antigen retrieval in boiling 1% citrate buffer for 15 min and then incubated with 0.3% hydrogen peroxide for 10 min to block endogenous peroxidase activity. The sections were incubated with protein block buffer at room temperature for 10 min to block nonspecific background staining. The sections were incubated with anti-HIF-1α antibody (1:500; Abcam, Cambridge, MA, USA; ab1) or anti-VEGF antibody (1:800; Abcam, Cambridge, MA, USA; ab46154) and then with biotinylated secondary antibody before illuminating in accordance with the manufacturer's instructions (Abcam; ab80436). The MOD was calculated to analyze the semiquantitative expression of HIF-1α and VEGF using Image-Pro plus 6.0 software. Two slices were randomly selected from each rat with six different areas as the detection field of view.

PA Analyses

PA analyses were completed 30 days after treatment. Rats were anesthetized with 1% sodium pentobarbital, and the hair around the bare joint was removed. An ultrasound and PA system (Vevo LAZR; FUJIFILM VisualSonic, Toronto, Ontario, Canada) were employed to acquire a vascular proliferative signal. A linear array transducer (LZ-400, 30 Hz) was utilized to obtain spatially coregistered ultrasound and PA. Light generated by a tunable laser operating at 808 nm for PA was delivered through fiber-optic bundles integrated into the transducer. The acquisition parameters, such as the gains of 28 dB for ultrasound images and 40 dB for PA, were constant for all of the imaging sessions. The MOD was calculated to analyze semiquantitatively the relative absorbance intensity of PA using Image-Pro plus 6.0 software.

Statistical Analysis

Data were statistically analyzed using one-way ANOVA SPSS 17.0 software to calculate p values. Results were expressed as mean ± standard deviation (SD), and statistical significance was considered at $p < 0.05$ (significant) and $p < 0.01$ (highly significant).

SUPPLEMENTAL INFORMATION

Supplemental Information can be found online at https://doi.org/10.1016/j.omtn.2020.01.014.

AUTHOR CONTRIBUTIONS

All authors were involved in drafting the article or revising it critically for important intellectual content, and all authors approved the final version to be published. Y.H. and P.Z. had full access to all of the data in the study and take responsibility for the integrity of the data and the accuracy of the data analysis. Study Conception and Design, P.Z., Y.H., L.Q., and Q.W.; Acquisition of Data, Y.H., T.Z., and Z.Z.; Analysis and Interpretation of Data, Y.H., Jianhai Chen, W.C., Jingqin Chen, J.L., G.Z., Y.Z., X.B., Y.W., and B.S.

CONFLICTS OF INTEREST

The authors declare no competing interests.

ACKNOWLEDGMENTS

This work was funded and supported by the National Key R&D Program of China (2018YFC1705205); Science and Technology Innovation Fund of Shenzhen (numbers JCYJ20170818153602439, JCYJ20160531174005444, JCYJ20180302150101316, JCYJ201708 18164059405, and JCYJ20170307112009204); SIAT Outstanding Youth Fund (Y5G002 and Y6G001); National Natural Science

Foundation of China (numbers NSFC81672224 and NSFC81473709); Sanming Project of Medicine in Shenzhen (number SZSM201808072; SZSM201612009); and Traditional Chinese Medicine Bureau of Guangdong Province (number 20183011).

REFERENCES

1. Jia, W., Wu, W., Yang, D., Xiao, C., Huang, M., Long, F., Su, Z., Qin, M., Liu, X., and Zhu, Y.Z. (2018). GATA4 regulates angiogenesis and persistence of inflammation in rheumatoid arthritis. Cell Death Dis. *9*, 503.
2. Xu, H., He, Y., Yang, X., Liang, L., Zhan, Z., Ye, Y., Yang, X., Lian, F., and Sun, L. (2007). Anti-malarial agent artesunate inhibits TNF-alpha-induced production of proinflammatory cytokines via inhibition of NF-kappaB and PI3 kinase/Akt signal pathway in human rheumatoid arthritis fibroblast-like synoviocytes. Rheumatology (Oxford) *46*, 920–926.
3. Gu, Q., Yang, H., and Shi, Q. (2017). Macrophages and bone inflammation. J. Orthop. Translat. *10*, 86–93.
4. Roman-Blas, J.A., and Jimenez, S.A. (2006). NF-kappaB as a potential therapeutic target in osteoarthritis and rheumatoid arthritis. Osteoarthritis Cartilage *14*, 839–848.
5. Mu, N., Gu, J., Huang, T., Zhang, C., Shu, Z., Li, M., Hao, Q., Li, W., Zhang, W., Zhao, J., et al. (2016). A novel NF-κB/YY1/microRNA-10a regulatory circuit in fibroblast-like synoviocytes regulates inflammation in rheumatoid arthritis. Sci. Rep. *6*, 20059.
6. Morita, T., Shima, Y., Fujimoto, K., Tsuboi, H., Saeki, Y., Narazaki, M., Ogata, A., and Kumanogoh, A. (2019). Anti-receptor activator of nuclear factor κB ligand antibody treatment increases osteoclastogenesis-promoting IL-8 in patients with rheumatoid arthritis. Int. Immunol. *31*, 277–285.
7. Thompson, C., Davies, R., and Choy, E. (2016). Anti cytokine therapy in chronic inflammatory arthritis. Cytokine *86*, 92–99.
8. Monaco, C., Nanchahal, J., Taylor, P., and Feldmann, M. (2015). Anti-TNF therapy: past, present and future. Int. Immunol. *27*, 55–62.
9. Chou, L.W., Wang, J., Chang, P.L., and Hsieh, Y.L. (2011). Hyaluronan modulates accumulation of hypoxia-inducible factor-1 alpha, inducible nitric oxide synthase, and matrix metalloproteinase-3 in the synovium of rat adjuvant-induced arthritis model. Arthritis Res. Ther. *13*, R90.
10. Brouwer, E., Gouw, A.S., Posthumus, M.D., van Leeuwen, M.A., Boerboom, A.L., Bijzet, J., Bos, R., Limburg, P.C., Kallenberg, C.G., and Westra, J. (2009). Hypoxia inducible factor-1-alpha (HIF-1alpha) is related to both angiogenesis and inflammation in rheumatoid arthritis. Clin. Exp. Rheumatol. *27*, 945–951.
11. Hirai, K., Furusho, H., Hirota, K., and Sasaki, H. (2018). Activation of hypoxia-inducible factor 1 attenuates periapical inflammation and bone loss. Int. J. Oral Sci. *10*, 12.
12. O'Neill, L.A., and Hardie, D.G. (2013). Metabolism of inflammation limited by AMPK and pseudo-starvation. Nature *493*, 346–355.
13. Losso, J.N., and Bawadi, H.A. (2005). Hypoxia inducible factor pathways as targets for functional foods. J. Agric. Food Chem. *53*, 3751–3768.
14. Cramer, T., Yamanishi, Y., Clausen, B.E., Förster, I., Pawlinski, R., Mackman, N., Haase, V.H., Jaenisch, R., Corr, M., Nizet, V., et al. (2003). HIF-1alpha is essential for myeloid cell-mediated inflammation. Cell *112*, 645–657.
15. Rius, J., Guma, M., Schachtrup, C., Akassoglou, K., Zinkernagel, A.S., Nizet, V., Johnson, R.S., Haddad, G.G., and Karin, M. (2008). NF-kappaB links innate immunity to the hypoxic response through transcriptional regulation of HIF-1alpha. Nature *453*, 807–811.
16. Hu, F., Liu, H., Xu, L., Li, Y., Liu, X., Shi, L., Su, Y., Qiu, X., Zhang, X., Yang, Y., et al. (2016). Hypoxia-inducible factor-1α perpetuates synovial fibroblast interactions with T cells and B cells in rheumatoid arthritis. Eur. J. Immunol. *46*, 742–751.
17. Hu, F., Mu, R., Zhu, J., Shi, L., Li, Y., Liu, X., Shao, W., Li, G., Li, M., Su, Y., et al. (2014). Hypoxia and hypoxia-inducible factor-1α provoke toll-like receptor signalling-induced inflammation in rheumatoid arthritis. Ann. Rheum. Dis. *73*, 928–936.
18. Berlow, R.B., Dyson, H.J., and Wright, P.E. (2017). Hypersensitive termination of the hypoxic response by a disordered protein switch. Nature *543*, 447–451.
19. Pouysségur, J., Dayan, F., and Mazure, N.M. (2006). Hypoxia signalling in cancer and approaches to enforce tumour regression. Nature *441*, 437–443.
20. Kunisch, E., Chakilam, S., Gandesiri, M., and Kinne, R.W. (2012). IL-33 regulates TNF-α dependent effects in synovial fibroblasts. Int. J. Mol. Med. *29*, 530–540.
21. Mo, X., Chen, J., Wang, X., Pan, Z., Ke, Y., Zhou, Z., Xie, J., Lv, G., and Luo, X. (2018). Krüppel-like factor 4 regulates the expression of inducible nitric oxide synthase induced by TNF-α in human fibroblast-like synoviocyte MH7A cells. Mol. Cell. Biochem. *438*, 77–84.
22. Hot, A., Zrioual, S., Lenief, V., and Miossec, P. (2012). IL-17 and tumour necrosis factor α combination induces a HIF-1α-dependent invasive phenotype in synoviocytes. Ann. Rheum. Dis. *71*, 1393–1401.
23. Lee, Y.A., Choi, H.M., Lee, S.H., Hong, S.J., Yang, H.I., Yoo, M.C., and Kim, K.S. (2012). Hypoxia differentially affects IL-1β-stimulated MMP-1 and MMP-13 expression of fibroblast-like synoviocytes in an HIF-1α-dependent manner. Rheumatology (Oxford) *51*, 443–450.
24. Fearon, U., Canavan, M., Biniecka, M., and Veale, D.J. (2016). Hypoxia, mitochondrial dysfunction and synovial invasiveness in rheumatoid arthritis. Nat. Rev. Rheumatol. *12*, 385–397.
25. Li, H., Fu, X., Gao, Y., Li, X., Shen, Y., and Wang, W. (2017). Small interfering RNA-mediated silencing of G-protein-coupled receptor 137 inhibits growth of osteosarcoma cells. J. Bone Oncol. *11*, 17–22.
26. Xiong, Y.S., Wu, A.L., Mu, D., Yu, J., Zeng, P., Sun, Y., and Xiong, J. (2017). Inhibition of siglec-1 by lentivirus mediated small interfering RNA attenuates atherogenesis in apoE-deficient mice. Clin. Immunol. *174*, 32–40.
27. Lund-Olesen, K. (1970). Oxygen tension in synovial fluids. Arthritis Rheum. *13*, 769–776.
28. Lee, Y.A., Kim, J.Y., Hong, S.J., Lee, S.H., Yoo, M.C., Kim, K.S., and Yang, H.I. (2007). Synovial proliferation differentially affects hypoxia in the joint cavities of rheumatoid arthritis and osteoarthritis patients. Clin. Rheumatol. *26*, 2023–2029.
29. Park, S.Y., Lee, S.W., Kim, H.Y., Lee, W.S., Hong, K.W., and Kim, C.D. (2015). HMGB1 induces angiogenesis in rheumatoid arthritis via HIF-1α activation. Eur. J. Immunol. *45*, 1216–1227.
30. Hollander, A.P., Corke, K.P., Freemont, A.J., and Lewis, C.E. (2001). Expression of hypoxia-inducible factor 1alpha by macrophages in the rheumatoid synovium: implications for targeting of therapeutic genes to the inflamed joint. Arthritis Rheum. *44*, 1540–1544.
31. Fan, M.P., Si, M., Li, B.J., Hu, G.H., Hou, Y., Yang, W., Liu, L., Tang, B., and Nie, L. (2018). Cell therapy of a knee osteoarthritis rat model using precartilaginous stem cells. Eur. Rev. Med. Pharmacol. Sci. *22*, 2119–2125.
32. Chuan-Ying, Y., and Lei, Z. (2012). Effects of shark cartilage polysaccharides on the secretion of IL-6 and IL-12 in rheumatoid arthritis. Pharm. Biol. *50*, 1567–1572.
33. Diarra, D., Stolina, M., Polzer, K., Zwerina, J., Ominsky, M.S., Dwyer, D., Korb, A., Smolen, J., Hoffmann, M., Scheinecker, C., et al. (2007). Dickkopf-1 is a master regulator of joint remodeling. Nat. Med. *13*, 156–163.
34. Smolen, J.S., Aletaha, D., Barton, A., Burmester, G.R., Emery, P., Firestein, G.S., Kavanaugh, A., McInnes, I.B., Solomon, D.H., Strand, V., and Yamamoto, K. (2018). Rheumatoid arthritis. Nat. Rev. Dis. Primers *4*, 18001.
35. Shabbir, A., Batool, S.A., Basheer, M.I., Shahzad, M., Sultana, K., Tareen, R.B., Iqbal, J., and Saeed-Ul-Hassan. (2018). Ziziphora clinopodioides ameliorated rheumatoid arthritis and inflammatory paw edema in different models of acute and chronic inflammation. Biomed. Pharmacother. *97*, 1710–1721.
36. Londhe, P., and Guttridge, D.C. (2015). Inflammation induced loss of skeletal muscle. Bone *80*, 131–142.
37. Wang, C.J., Cheng, J.H., Chou, W.Y., Hsu, S.L., Chen, J.H., and Huang, C.Y. (2017). Changes of articular cartilage and subchondral bone after extracorporeal shockwave therapy in osteoarthritis of the knee. Int. J. Med. Sci. *14*, 213–223.
38. Adeneye, A.A., Oreagba, A.I., Ishola, I.O., and Kalejaiye, H.A. (2014). Evaluation of the anti-arthritic activity of the hydroethanolic leaf extract of Alchornea cordifolia in rats. Afr. J. Tradit. Complement. Altern. Med. *11*, 402–410.
39. Patil, K.R., Patil, C.R., Jadhav, R.B., Mahajan, V.K., Patil, P.R., and Gaikwad, P.S. (2011). Anti-Arthritic Activity of Bartogenic Acid Isolated from Fruits of

Barringtonia racemosa Roxb. (Lecythidaceae). Evid. Based Complement. Alternat. Med. *2011*, 785245.

40. Ashraf, S., Mapp, P.I., and Walsh, D.A. (2010). Angiogenesis and the persistence of inflammation in a rat model of proliferative synovitis. Arthritis Rheum. *62*, 1890–1898.

41. Feng, Z.T., Yang, T., Hou, X.Q., Wu, H.Y., Feng, J.T., Ou, B.J., Cai, S.J., Li, J., and Mei, Z.G. (2019). Sinomenine mitigates collagen-induced arthritis mice by inhibiting angiogenesis. Biomed. Pharmacother. *113*, 108759.

42. Deng, Q., Bai, S., Gao, W., and Tong, L. (2015). Pristimerin inhibits angiogenesis in adjuvant-induced arthritic rats by suppressing VEGFR2 signaling pathways. Int. Immunopharmacol. *29*, 302–313.

43. Thairu, N., Kiriakidis, S., Dawson, P., and Paleolog, E. (2011). Angiogenesis as a therapeutic target in arthritis in 2011: learning the lessons of the colorectal cancer experience. Angiogenesis *14*, 223–234.

44. Arjamaa, O., Aaltonen, V., Piippo, N., Csont, T., Petrovski, G., Kaarniranta, K., and Kauppinen, A. (2017). Hypoxia and inflammation in the release of VEGF and interleukins from human retinal pigment epithelial cells. Graefes Arch. Clin. Exp. Ophthalmol. *255*, 1757–1762.

45. Lu, Y., Yu, S.S., Zong, M., Fan, S.S., Lu, T.B., Gong, R.H., Sun, L.S., and Fan, L.Y. (2017). Glucose-6-Phosphate Isomerase (G6PI) Mediates Hypoxia-Induced Angiogenesis in Rheumatoid Arthritis. Sci. Rep. *7*, 40274.

46. Brand, D.D., Latham, K.A., and Rosloniec, E.F. (2007). Collagen-induced arthritis. Nat. Protoc. *2*, 1269–1275.

47. Lin, H.S., Hu, C.Y., Chan, H.Y., Liew, Y.Y., Huang, H.P., Lepescheux, L., Bastianelli, E., Baron, R., Rawadi, G., and Clément-Lacroix, P. (2007). Anti-rheumatic activities of histone deacetylase (HDAC) inhibitors in vivo in collagen-induced arthritis in rodents. Br. J. Pharmacol. *150*, 862–872.

48. Hu, Y., Li, J., Qin, L., Cheng, W., Lai, Y., Yue, Y., Ren, P., Pan, X., and Zhang, P. (2016). Study in Treatment of Collagen-Induced Arthritis in DBA/1 Mice Model by Genistein. Curr. Pharm. Des. *22*, 6975–6981.

49. Tomita, T., Takeuchi, E., Tomita, N., Morishita, R., Kaneko, M., Yamamoto, K., Nakase, T., Seki, H., Kato, K., Kaneda, Y., and Ochi, T. (1999). Suppressed severity of collagen-induced arthritis by in vivo transfection of nuclear factor kappaB decoy oligodeoxynucleotides as a gene therapy. Arthritis Rheum. *42*, 2532–2542.

OMTN, Volume *19*

Supplemental Information

Downregulation of Hypoxia-Inducible Factor-1α by RNA Interference Alleviates the Development of Collagen-Induced Arthritis in Rats

Yiping Hu, Tiantian Zhang, Jingqin Chen, WenXiang Cheng, Jianhai Chen, Zhengtan Zheng, Jietao Lin, Guoyuan Zhu, Yong Zhang, Xueling Bai, Yan Wang, Bing Song, Qingwen Wang, Ling Qin, and Peng Zhang

Supplementary Material for

Down-regulation of hypoxia-inducible factor-1α by RNA interference alleviates the development of collagen-induced arthritis in rats

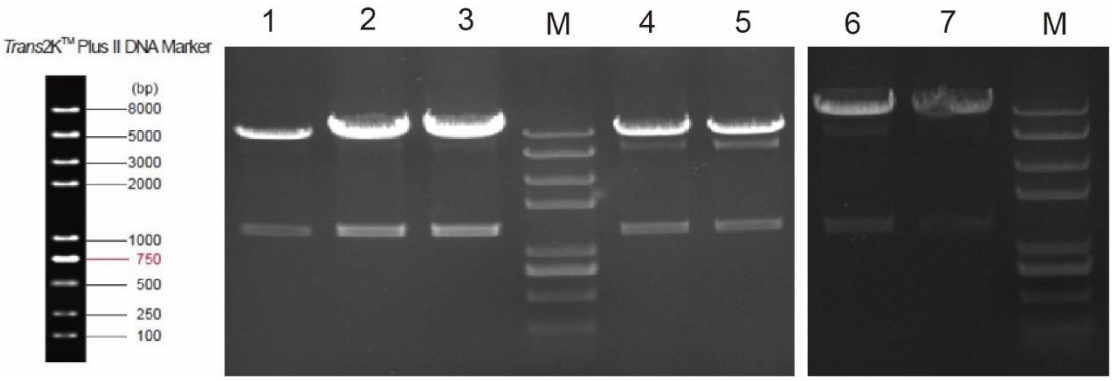

Figure S1. The pLVX-shRNA-HIF-1α plasmid digested and identified by XhoI enzyme. Lane M: Trans2K plus marker, Lane 1,2,3: pLVX-shRNA1-HIF-1α digested by XhoI, Lane 4,5: pLVX-shRNA2-HIF-1α digested by XhoI, Lane 6,7: pLVX-shRNA3-HIF-1α digested by XhoI

Figure S2. Vector plasmid sequencing (A) pLVX-shRNA1-HIF-1α, (B) pLVX-shRNA2-HIF-1α,

(C) pLVX-shRNA3-HIF-1α.

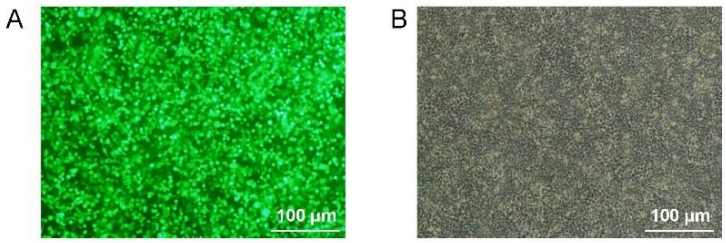

Figure S3. 24 h green fluorescence after transfection，(A) Green fluorescence observation after transfection of 293T cells for 24h, (B) Control non-fluorescent cell

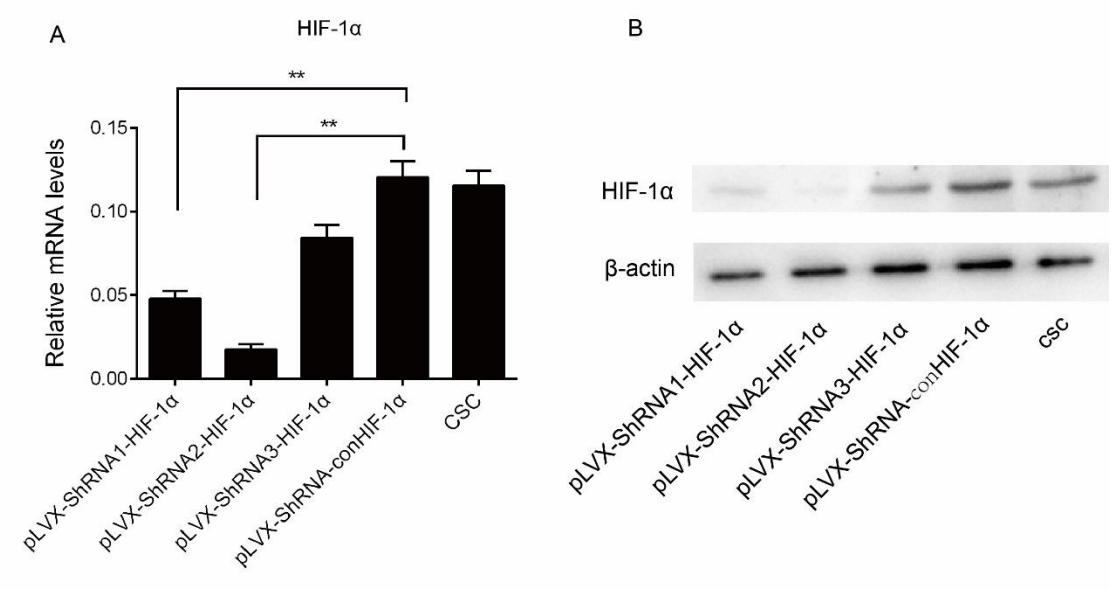

Figure S4. HIF-1α silencing effectiveness analysis, (A) HIF-1α mRNA expression, (B) HIF-1α Protein expression

Methods

shRNA design, viral packaging and its effectiveness screening

(1) We designed 3 pairs of shRNAs that target HIF-1, and the sense and antisense sequences are as follows:

rHIF-lα-shRNA1-F：
5′-GATCCGCAGTGTGGCTACAAGAAACCTTCAAGAGAGGTTTCTTGTAGCCACACTGCTTTTTTCTCGAGG-3′
rHIF-lα-shRNA1-R：
5′-AATTCCTCGAGAAAAAAGCAGTGTGGCTACAAGAAACCTCTCTTGAAGGTTTCTTGTAGCCACACTGCG-3′
rHIF-lα-shRNA2-F：
5′-GATCCGCATTGAAGTTAGAGTCAAGCTTCAAGAGAGCTTGACTCTAACTTCAATGCTTTTTTCTCGAGG-3′

rHIF-lα-shRNA2-R：
5′-AATTCCTCGAGAAAAAAGCATTGAAGTTAGAGTCAAGCTCTCTTGAAGC
TTGACTCTAACTTCAATGCG-3′
rHIF-lα-shRNA3-F：
5′-GATCCGCAGTGACGAAGGACAATATATTCAAGAGATATATTGTCCTTCGT
CACTGCTTTTTTCTCGAGG-3′
rHIF-lα-shRNA3-R：
5′-AATTCCTCGAGAAAAAAGCAGTGACGAAGGACAATATATCTCTTGAATA
TATTGTCCTTCGTCACTGCG-3′

(2) The pLVX-shRNA-HIF-1α plasmid was constructed and extracted in large amounts using a plasmid extraction kit, and then digested and identified by XhoI enzyme (Figure S1).

(3) Vector plasmid sequencing

Sequencing is done by commercial companies (Figure S1)**.**

(4) Fluorescence observation of virus packaging and transfection of 293T cells for 24h (Figure S3)

(5) Detection of the effectiveness of synovial cell silencing HIF-1α

The detailed operation of real time-PCR and western blot analysis are described in the text (Figure S4).